Non-linear soil response to strong ground motion: Determinations based on SASW velocity profiles

Siasi Kociu (kocius@umr.edu), Ronaldo Luna (rluna@umr.edu), Neil Anderson (nanders@umr.edu), Wei Zheng (wzheng@umr.edu), and *Dave Hoffman (nrhoffd@mail.dnr.state.mo.us)

University of Missouri-Rolla
*MoDNR, Geological Survey & Resource Assessment:

Abstract

Cross-borehole compression and shear-wave velocity control (to depths on the order of 70 m) were acquired at two separate bridge sites in southeast Missouri. SASW data were also acquired at each site, and used to generate subsurface velocity profiles to depths on the order of 70 m. The cross-borehole and SASW velocity profiles correlate well, indicating that the non-invasive and less expensive SASW technique can be used with confidence in the study area. Synthetic strong ground motions at bedrock were generated at each bridge site using point source models. These ground motions were propagated to the earth's surface assuming soil response was linear at depths greater than 60 m, and non-linear at depths shallower than 60 m. The non-linear soil response at each bridge site was estimated on the basis of the respective shear-wave velocity profiles.

Introduction

The New Madrid Seismic Zone (NMSZ) represents the most hazardous seismic zone in the central and eastern US. The great earthquakes of 1811-1812 with moment magnitudes M_w=7.5-8.0 caused extensive ground failures (especially liquefaction), and evidence of this phenomena can be seen even today on satellite images. The great thickness of the soil sediments has been the focus of research to study the amplification or de-amplification given input strong ground motions with PGA>0.4g due to degradation of shear moduli and increase of strains in depth [8, 9]. These conclusions were included in FEMA Reports [3, 4]

The sites under investigations are located in the NMSZ on the Mississippi embayment, which are characterized by very thick sediments (730-780m) overlying the Paleozoic rock. The upper part of these deep sediments (80m) consists of very poor Quaternary deposits, studied by SASW and cross-hole techniques [1]. As there are no strong motion records in this area, therefore synthetic ground motions were used.

This paper focuses on the engineering significance of the geophysical method used for the purpose ground response analysis. It was originally hypothesized that the resolution and quality of SASW data would be sufficient for the purpose of ground response analysis in shallow and deep soil deposits such as the ones present in the NMSZ.

1. Synthetic ground motions used as input - Point source model:

1.1. Geotectonic model

The Bridges sites under investigation are situated on the top of thick sediments overlying the Reelfoot Rift [11] in New Madrid Zone .The bridges are part of the located along I-55 in the southeast corner of the state of Missouri near the cities of Hayti and Steele.

1.2. Depth to bedrock

For the determination of the depth to Paleozoic bedrocks the data from MoDNR were used (see Table 1.1).

Table.1.1.Estimated Geologic Profile at Bridge Sites[7]

Bridge Site (1)	(2)	(3)	(4)	(5)	(6)	(7)	(8)	(9)	(10)	(11)	(12)	(13)	(14)
L-472	80	25	55	55	25	55	725	-700	780	6300	-7000	7080	20
A-1466	80	25	55	55	25	55	675	-650	730	5350	-6000	6080	20

Notes:
2. Ground surface approximate elevation (m)
3. Base of Unconsolidated Alluvium Approximate Elevation (m)
4. Approximate Depth to Base of Unconsolidated Alluvium (m)
5. Approximate Thickness of Unconsolidated Alluvium (m)
6. Top of Unconsolidated Tertiary& Cretaceous Sediments (m)
7. Approximate Depth to Top of Unconsolidated Tertiary& Cretaceous Sediments. Approximate Elevation in (m)
8. Approximate Thickness of Unconsolidated Tertiary & Cretaceous Sediments (m)
9. Top of Paleozoic Bedrock. Approximate Elevation (m)
10. Approximate Depth to Top of Paleozoic Bedrock (m)
11. Approximate Thickness of Paleozoic Bedrock (m)
12. Top of Precambrian Basement (m)
13. Approximate Depth to Top of Precambrian Basement (m)
14. Approximate Bottom of Seismogenic Crust (km)

The thickness of soil layer on the top of hard Paleozoic rocks was derived from the data supplied by MoDNR (see Table 1.1):

- Top of Paleozoic bedrock at depths: h=-700 m for L-472) and h=-650m for A-1466
- Thickness of consolidated sediments: H=700 m (L-472), H=650m (A-1466)
- Approximate thickness of unconsolidated alluvium and Tertiary sediments:
- H=55+25=80m (L-472), H=55+25=80m(A-1466)

Therefore the strong ground motions generated by the Reelfoot Rift may be modified by the thick sediments on the top of Paleozoic rocks of the thickness 650-700m, behaving linearly; and the poor soil sediments of the upper part of cross sections of the thickness 70-80m behaving nonlinearly. Synthetics used as input motions were generated at the top of consolidated sediments overlying the Paleozoic bedrock.

1.3. Shear wave velocity (V_s) models:

For the generation of synthetic ground motions the velocity models for Mid-America & NMSZ according to the inversion of teleseismic data were used [5]. The preliminary sediment thickness for the model was 1000m thick were used for New Madrid Seismic Zone (see Table 1.2).

1.4. Strong motion parameters according to seismic hazard maps

The USGS 1996 seismic hazard maps for PE=2% in T=50yrs by entering a latitude and longitude for two bridge sites at the website of National Seismic Hazard Mapping Project[15] were used to find the corresponding seismic hazard parameters (Table 1.4). For the generation of synthetics, the modified Mid-America Deep Soil USGS96 source model was used (see Table 1.3)

Table 1.2.Prototype Model [5]

Layer	**Material**	**Thickness** (m)	**Vp** (m/s)	**Vs** (m/s)	Density gm/cc	**Qp**	**Qs**
1	Soil	0-2000	1800	$250\ h^{0.18}$	$0.8\log_{10}Vs-0.1$	$6\ h^{0.24}$	$6\ h^{0.24}$
2	Upper Paleozoic	500	4500	2500	2.5	500	500
3	Lower Paleozoic	500	5000	3000	2.6	500	500
4	Precambrian	-	6000	3500	2.7	500	500

Table 1.3.Mid-America Ground Motion Models used for the generation of synthetics [6]

Model	**Name**	**Source**	**Wave propagation**	**Site effects**
5(M5)	Mid-America Deep Soil USGS96source (modified)	USGS 96 150 bar	Mid-America	Mid-Continent Deep Soil

Table 1.4: Seismic hazard parameters for bridge sites

Parameters	**Bridge Site A-1466** (36°22N 89°74W)	**Bridge Site L-472** (36°10N 89°78W)
PGA (g)	1.510068	1.475792
0.2sec Sa (g)	3.105915	3.001929
0.3sec Sa (g)	2.526520	2.465689
1.0sec Sa (g)	0.982504	0.960957

The distances and magnitudes used to calculate these hazard values were found according to the USGS special tables for PGA, 02.sec S_a, 0.3 sec S_a and 1.0 sec S_a, as functions of log (km) and moment magnitude (M_W)**.** To generate synthetics for both bridge sites three combinations of parameters were chosen, as shown below:

D=10km & M_W=7.1

D=16km & M_W=7.8

D=20km & M_W=8.1

1.5. Computer codes

For the generation of synthetics was used the Boore's SMSIM package [2]:

- Program *dorvt180* to create a standard set of parameter files using as input data:
  - M, d (km), h (m), number of simulations and seed number.
- Program ***td_drvr*** and *rv_drvr* to compute acceleration time history, peak ground motions (PGA, PGV, PGD) and response spectra for a given damping (5%).

1.6. Synthetics generated for A-1466 Bridge Site

1.6.1. Synthetics for h=0m (on the top of Paleozoic rocks)

It is common for the generation of synthetics on hard rocks to set the thickness of the overlying layer to h=0m. As an example 3 synthetics are presented for the same seed to generate the synthetics (S=123) for different magnitudes and distances *(see Table 1.5. and Figure 1.3 b)

Table 1.5 - Synthetics on hard rocks for A-1466 Bridge Site

Synthetics	M	D (km)	Seed	PGA (g)
1D	7.1	10	123	1.6799
6D	7.8	16	123	2.1274
11D	8.1	20	123	1.9572

1.6.2. Dependence of parameters of synthetics on thickness of sediments h (m)

During the generation of synthetics it was observed that the thickness of soil layers on the top of Paleozoic rocks (h) influences the PGA values and values of response acceleration spectra for the same model. In Figure 1.1, the dependence of PGA values for synthetics generated at varying magnitudes of h (m) values using the ModelM5 for M=7.1, D=10km, and a seed of 123. From this figure it can be seen the decrease 2 times of PGA on free surface. Figure 1.2 shows how the thickness of soil or overburden on top of rock affects the response spectra of the rock motion. The spectra are shown as 5% damping for the different thickness.

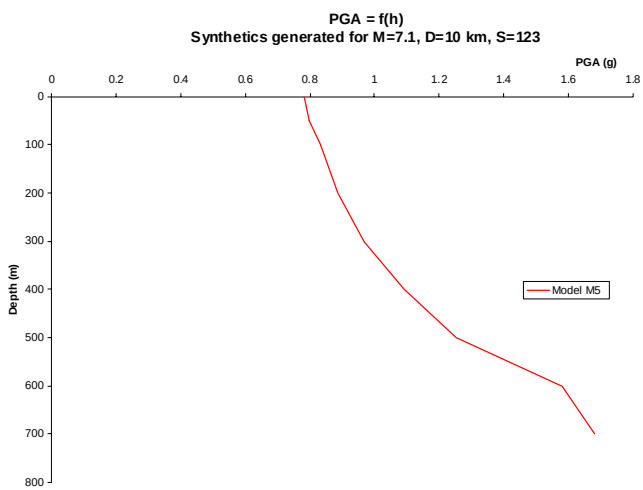

Figure 1.1. PGA values (g) in different depths for synthetics (Model M5 for M=7.1,D=10km, S=123)

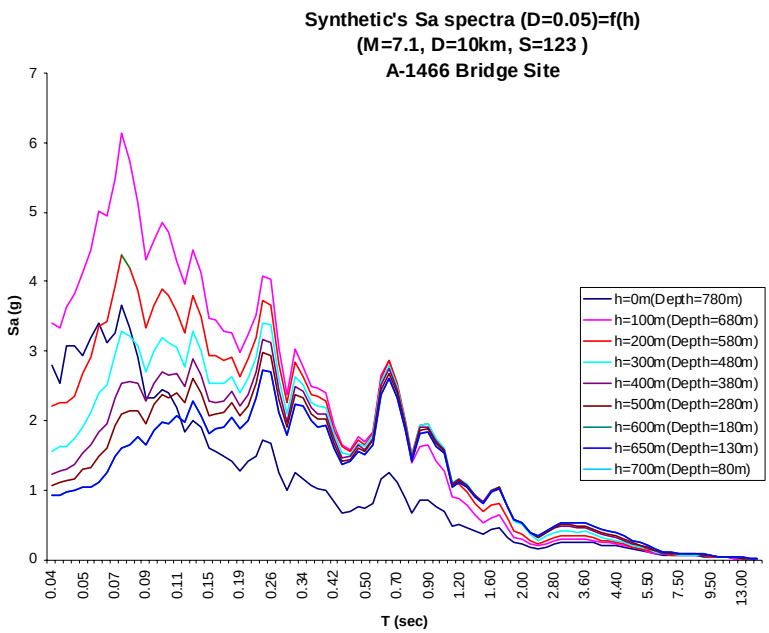

Figure 1.2. Sa spectra (D=0.05) in different depths for synthetics (Model M5 for M=7.1,D=10km, S=123)

From this figure it can be seen that for the same model (M=7.1, D=10km, S=123) the peak spectral acceleration response shifts to the longer periods and decreasing as values with increasing of the thickness of soil layers on the top of Paleozoic rock.

1.6.3. Synthetics for A-1466 Bridge Site (h=650m)

As the thickness of soils on the top of Paleozoic rocks underneath bridge site A-1466 is about 730m, excluding the upper part of poor soils of 80m thick, synthetics were generated for the thickness h=730-80=650m according to Boore's programs [2]. Acceleration time histories and velocity time histories were computed for 5 different seeds (123, 1234, 2345, 345, and 78) for each of three combinations of distances and magnitudes were generated 15 synthetics. (See Table 1.6).

According to these time histories it can be seen that PGA & PGV values for 15 synthetics for each bridge site are very close to each other (see figure 1.3a,b). Response acceleration spectra for 5% damping value are presented in the figure 1.4 and 1.5. In the figure 1.5 it can be seen that average values of the response acceleration spectra for 5 random values for different combination of M_w and D (km) are close to each other with the lowest values for M_w=7.1,D=10km and the highest one for M_w=7.8, D=20km.

1.7. Determination of the level of input motions

Based on above mentioned synthetics it can concluded that:

1. PGA average values of input motions can be presented as follows:
    - For the bridge site A-1466: PGA_{av}=0.99-1.16g
    - For the bridge site L-472: PGA_{av}=0.98-1.15g
2. The increase of the thickness of sediments on the top of Paleozoic rocks by 50 meters (L-472) has a very small influence on the mean average value (only 0.01g less)

Synthetics	M_w	D (km)	Seed	PGA (g)	Average PGA
S_1	7.1	10	123	.783	0.992
S_2	7.1	10	1234	1.158	
S_3	7.1	10	2345	1.005	
S_4	7.1	10	345	0.958	
S_5	7.1	10	78	1.059	
S_6	7.8	16	123	1.173	1.154
S_7	7.8	16	1234	1.071	
S_8	7.8	16	2345	1.049	
S_9	7.8	16	345	1.012	
S_{10}	7.8	16	78	1.466	
S_{11}	8.1	20	123	1.274	1.161
S_{12}	8.1	20	1234	1.162	
S_{13}	8.1	20	2345	1.081	
S_{14}	8.1	20	345	0.947	
S_{15}	8.1	20	78	1.340	

Table 1.6 Parameters of synthetics for A-1466 bridge site

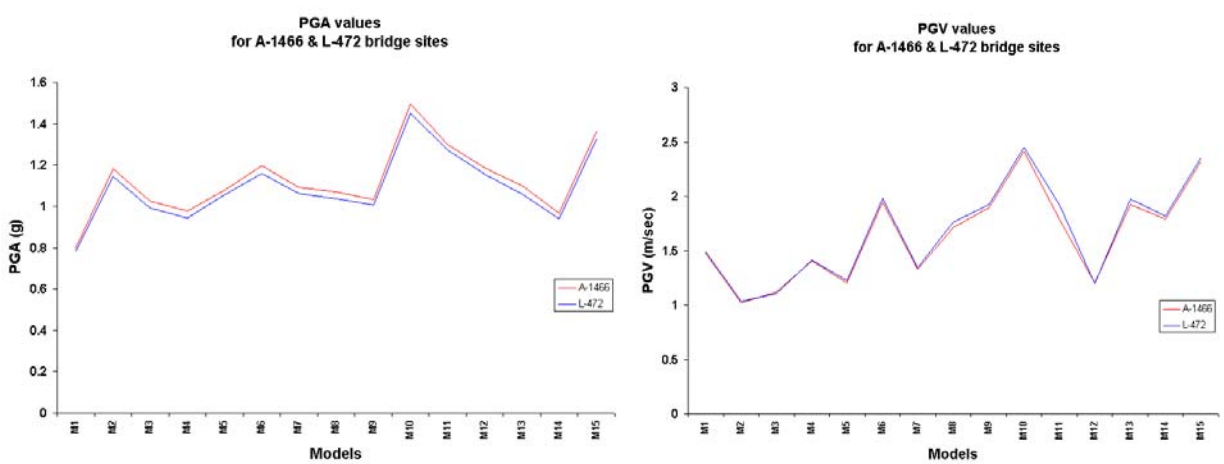

a) b)

Fig.1.3.PGA (a) and PGV (b) values for 15 synthetics

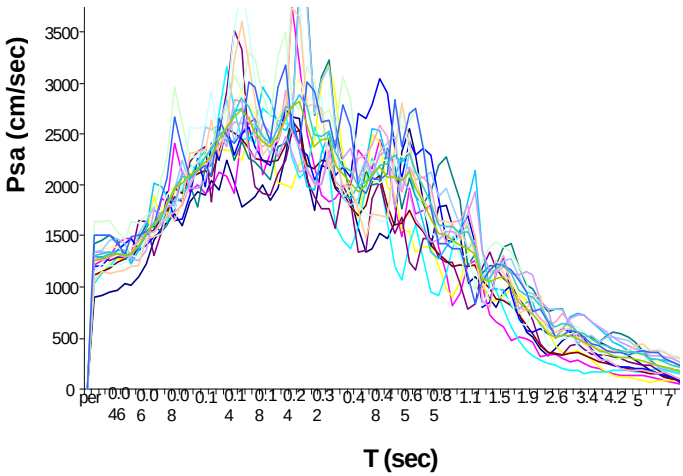

Figure 1.4. Response acceleration spectra for 15 synthetics

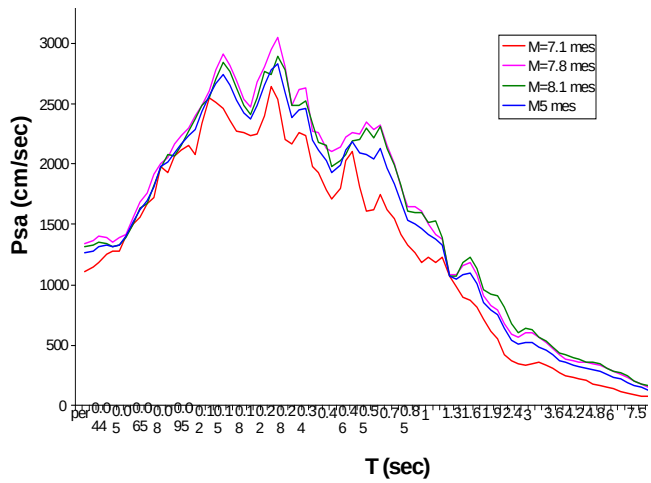

Figure.1.5 Comparison of average Sa spectra for 3 combinations of M_w and D (km)

2. Non-linear soil response analysis of the upper part of soil profiles:

At the level of input motion, top of Paleozoic rock at about 650-700m the input PGA was determined as 1.0g (for A-1466 and L-472 bridge site) the influence of the nonlinear response of sediments of the upper part of the thickness around 80m is pronounced. However, at depths below the response is for the most part one of elastic response.

2.1. Soil profiles based on shear wave velocity data.

The soil profiles of the bridge sites were compiled using geologo-lithological data and shear wave velocity data from two sources: cross-hole (CH) data and Rayleigh surface wave or Spectral Analysis of Surface Waves (SASW) data. For bridge site L-472 (Figure.2.1) the SASW testing was performed nearby the location where a seismic cone penetrometer (SCPT) was previously advanced. For the bridge site A-1466 (Figure.2.2) both SASW and cross-hole data were acquired in addition to the SCPT data at that site.

2.2. Soil profile of the bridge site A-1466

The one-dimensional geotechnical model for A-1466 bridge site was compiled taking into account the borehole data concerning lithology of the upper part of the cross section (layers 1-3) and Vs data according to SASW technique. It has to be mentioned that the Vs value of 250 m/sec for the 3-d and 4-th layers coincide with Vs value found by Liu and alias [13](from 8-32m). For the lower part the data from the generalized model presented in the table 1.3 were accepted.
The unit weight values for the upper part of cross-sections were computed based on well-known relationships [6].

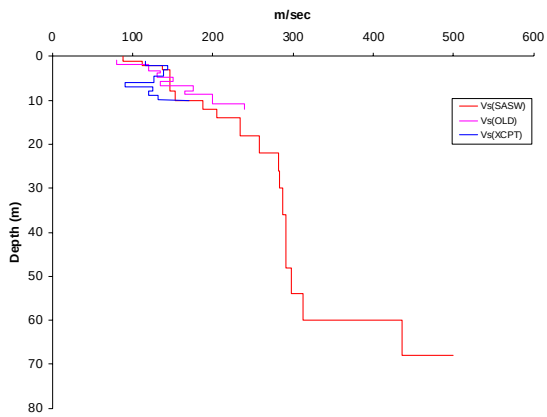

Fig.2.1.Shear wave's profile (bridge L-472)

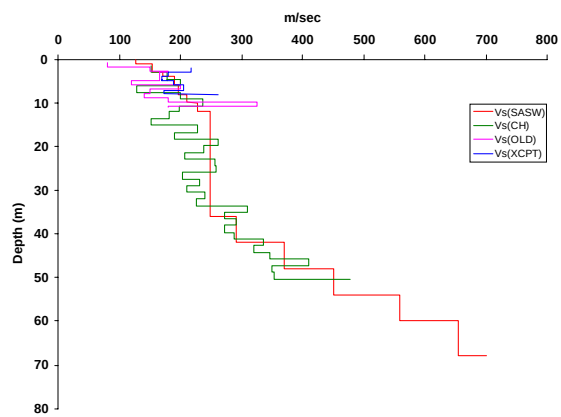

Fig.2.2.Shear wave's profile (bridge A-1466)

Table 2.1.One dimensional geotechnical model for A-1466 bridge site using SASW and cross-hole (CH) characterization techniques

Layer	**Lithology**	**SASW data**				**CH data**			
		Thickness (m)	**Depth** (m)	**Vs** SASW m/sec	**ρ** T/m^3	Thickness (m)	Depth (m)	**Vs** CH m/sec	**ρ** T/m^3
1	Mostly brown sandy silt to silty sand	3.0	3.0	142	1.43	3.05	3.05	137	1.42
2	Gray, stiff to very stiff sandy silt to silty sand	8.57	11.6	200	1.54	8.75	11.8	153	1.46
3	Mostly dense to very dense fine sand	10.0	21.6	250	1.62	10.7	22.5	190	1.52
4	Mostly dense to very dense fine sand	14.0	35.6	250	1.62	13.7	36.2	250	1.62
5	Mostly dense to very dense fine sand	6	41.6	290	1.68	6	42.3	305	1.69
6		6	47.6	365	1.76	6.1	48.4	310	1.70
7		6	53.6	450	1.85	5.2	53.6	390	1.79

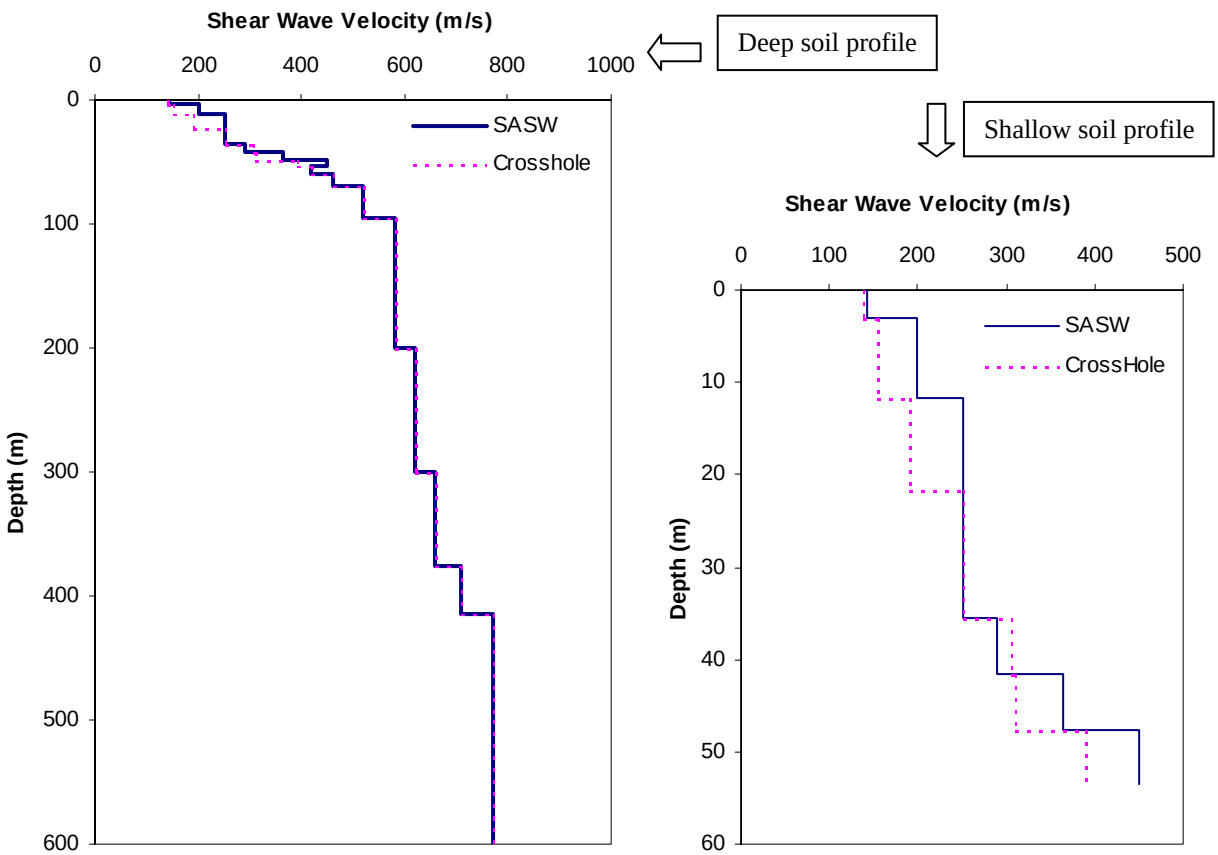

Fig.2.3. Deep and Shallow soil profiles used in analyses (bridge A-1466).The extrapolation of Vs SASW values for deep soil profile beneath 80 m was done according to [5,13]

2.3. Input motions

Input motions were considered by developing three synthetics for h=0m (on the top of Paleozoic hard rocks) and another three synthetics for h=650m. However, for the purpose of comparing the SASW and the CH significance in ground response only one ground motion was used as highlighted in Table 2.2). The input motion used in the comparative analysis was for a magnitude of 7.1g.

Table 2.2.Synthetics for New Madrid Seismic Zone

Synthetics h=650m	**M**	**D (km)**	**Seed**	**PGA** (g)	**Synthetics h=0m**	**M**	**D** (km)	**Seed**	**PGA** (g)
1	7.1	10	123	0.783	1D	7.1	10	123	1.6799
6	7.8	16	123	1.173	6D	7.8	16	123	2.1274
11	8.1	20	123	1.274	11D	8.1	20	123	1.9572

As can be seen from the table 2.2 PGA values of synthetics generated on the top of Paleozoic hard rocks (S1D, S6D, S11D) are 1.5-2 times greater that PGA values of synthetics generated for h=650m (S1, S6, S11)(See Figure 2.4)

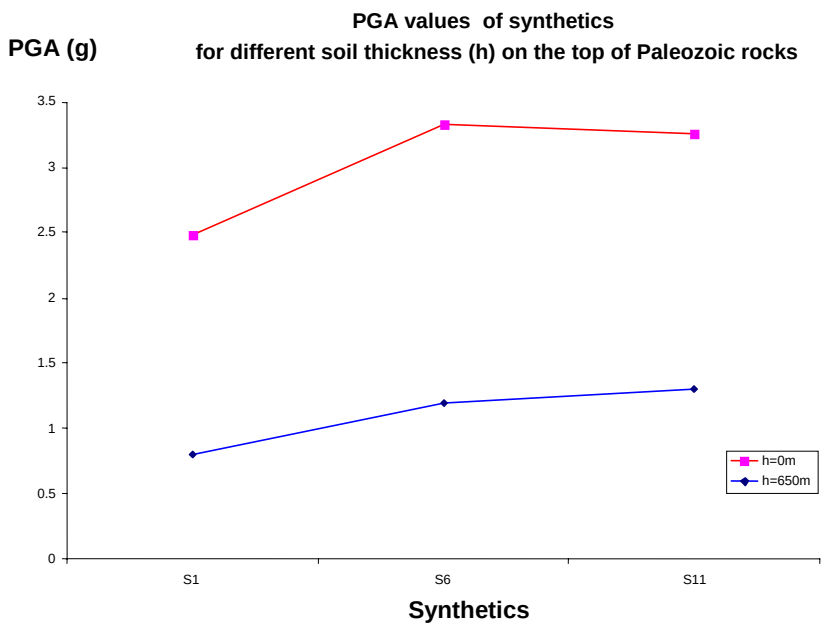

Figure 2.4. Dependence of PGA values for synthetics generated for different thickness (h) of soil layers on the top of Paleozoic rocks.

Taking into consideration the shape of response acceleration spectra (D=0.05) is different The highest response is observed in the range of shorter periods (0.04-0.16sec) for synthetics generated on the top of hard rocks (h=0m), meanwhile for synthetics generated for h=650m it is observed in the range of medium periods (0.25-0.55sec) (See Figure 2.5)

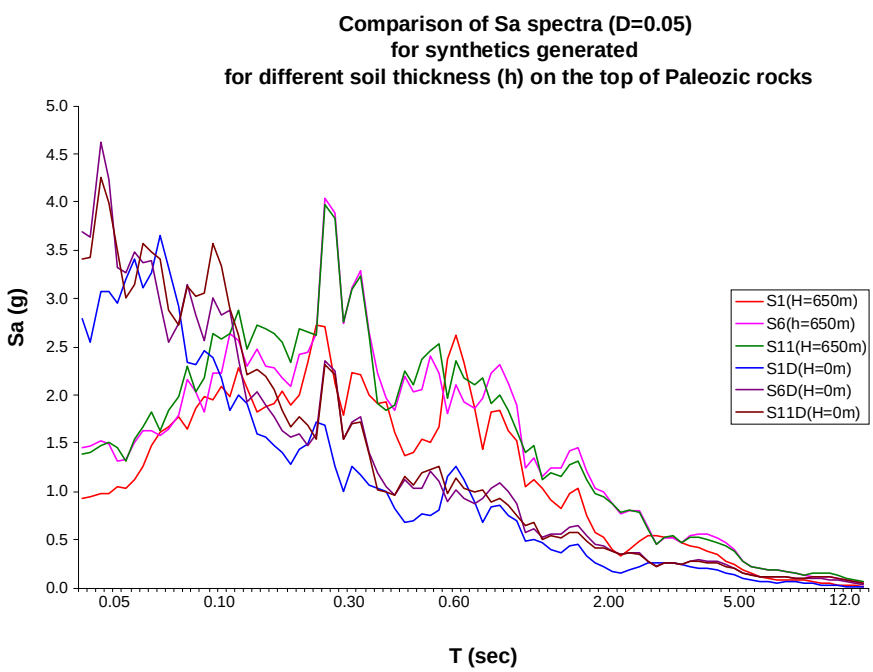

Fig.2.5.Sa spectra (D=0.05) for synthetics generated for different soil thickness (h) on the top of Paleozoic rocks

2.4. Ground Response Analyses & Computer code

Generally, real seismic waves generated from an earthquake are propagated in a three-dimensional continuous medium. However, modeling the nonlinear soil behavior as well as the three-dimensional wave propagation is extremely difficult and computationally intensive. In most situations the main response in the soil deposit can be adequately approximated with one or two-dimensional vertical propagation of shear waves.

This paper proposes a nonlinear two-dimensional soil model in the time domain. In this approach, equations of motion and equilibrium are solved in discrete time increments, which represent the nonlinear behavior of soil under the earthquake loading. The analysis of dynamic site response requires solving the global dynamic equation of motion given by the following equation in matrix form:

$$[M]\{\ddot{u}\}+[C]\{\dot{u}\}+[K]\{u\}=P(t) \qquad (2.4.1)$$

where $[M]$, $[C]$ and $[K]$ are the global mass, damping and stiffness matrices for assemblage of elements, respectively; $\{\ddot{u}\}$, $\{\dot{u}\}$ and $\{u\}$ are the relative nodal acceleration, velocity and displacement vectors and $P(t)$ is the load vector, which for base excitation can be written as:

$$P(t)=-[M]\{I\}\ddot{u}_g(t) \qquad (2.4.2)$$

where, $\{I\}$ is the identity vector and $\ddot{u}_g(t)$ is the input base acceleration time history. The $[M]$, $[C]$ and $[K]$ matrices are assembled using an incremental approach and are updated at every time step. The direct integration method – Newmark method [16] is used to solve Eq. (2.4.1).

The dynamic soil properties – the shear modulus and the damping ratio are obtained from the published unified formulas obtained by fitting the experimental curves [10]. The formulas take into account the effect of the effective confining pressure, the plasticity index of the soil and the shear strain level to the shear modulus degradation curve and the damping ratio curve, which can be expressed in the following form:

$$G/G_{\max}=K(\gamma,PI)(\overline{\sigma}_0^{'})^{m(\gamma,PI)} \qquad (2.4.3)$$

where, $G_{\max}$ is the initial shear modulus; γ is the shear strain; G is the shear modulus at the shear strain γ; PI is the plasticity index of the soil; $\overline{\sigma}_0^{'}$ is the mean effective confining pressure. Based on the plasticity index, K and m are two functions used to control the shape of the shear modulus degradation curve, which can be written as:

$$K(\gamma,PI)=0.5\left\{1+\tanh\left[\ln\left(\frac{0.000101+n(PI)}{\gamma}\right)^{0.492}\right]\right\} \qquad (2.4.4)$$

$$m(\gamma,PI)=0.272\left\{1-\tanh\left[\ln\left(\frac{0.000556}{\gamma}\right)^{0.4}\right]\right\}e^{(-0.0145PI^{1.3})} \qquad (2.4.5)$$

where, n is a coefficient to consider the influence of the plasticity index to the degradation curve, which can be determined:

$$n(PI)=\begin{Bmatrix} 0.0 & for \quad PI=0 \\ 3.37\times10^{-6}PI^{1.404} & for \quad 0<PI\le15 \\ 7.0\times10^{-7}PI^{1.976} & for \quad 15<PI\le70 \\ 2.7\times10^{-5}PI^{1.115} & for \quad PI>70 \end{Bmatrix} \qquad (2.4.6)$$

The shear modulus degradation curve presented from Eq. (2.4.3)~(2.4.6) can be described as the backbone curve in stress-strain field. An example is shown in Fig. 2.6. Fig. 2.6(a) shows the modulus degradation curve for sand at the confining pressure $\bar{\sigma}_0^{'}$ equal to 100 kpa. Fig. 2.6(b) shows the corresponding backbone curve when the maximum shear modulus $G_{\max}$ is 20 MPa. The backbone curve from the unified formulas is also compared with that from the hyperbolic model in Fig. 2.5(b). The hyperbolic stress-strain relationship initially formulated by Konder and Zelasko [12] can be expressed as below:

$$\tau = \frac{G_{\max}\gamma}{1+\frac{G_{\max}}{\tau_{\max}}|\gamma|} \qquad (2.4.7)$$

where, τ is the shear stress at strain amplitude γ; and $\tau_{\max}$ is the maximum shear stress that can be applied to the sand in its initial state without failure.

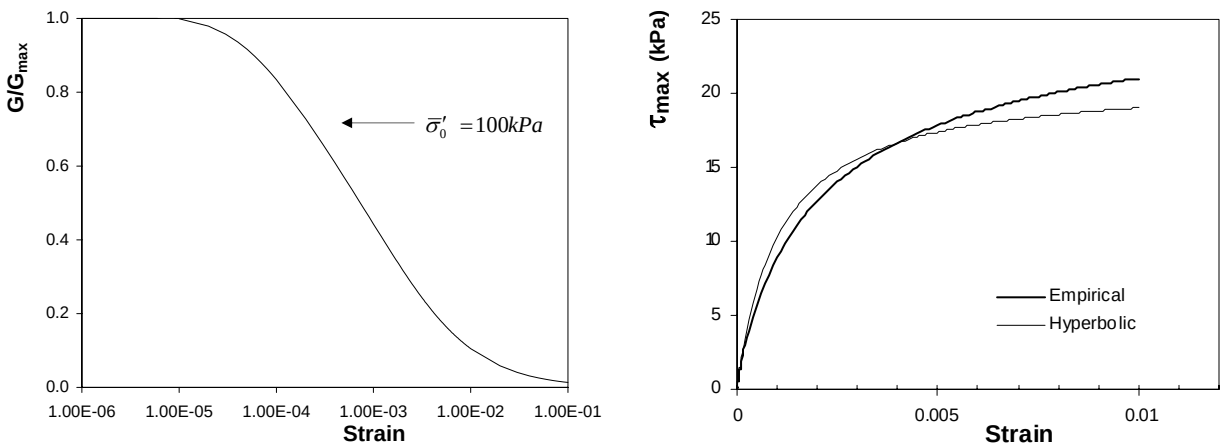

(a) (b)

Fig. 2.6. (a) Modulus Degradation Curve for Sand; (b) Corresponding Backbone Curve

The extended Masing criteria [14] are used to govern the unloading-reloading behavior of soil. The detail of the rules are described below (shown in Fig. 2.7):

- For initial loading, the stress-strain curve follows the backbone curve described above.
- If a stress reversal occurs at a point defined by (γ_r, τ_r), the reloading or unloading stress-strain curve follows a path given by

$$(\tau - \tau_r)/2 = f\left(\frac{\gamma - \gamma_r}{2}\right) \qquad (2.4.8)$$

where, *f* represents the function for describing the backbone curve. Basically, the unloading and reloading curves have the same shape as the backbone curve (with the origin shifted to the loading reversal point), but are enlarged by a factor of 2. For this model, $(\gamma - \gamma_r)/2$ is used to replace γ in Eq. (2.4.3) ~ (2.4.6) to calculate the shear modulus ratio $G/G_{\max}$ for the unloading and reloading behavior.

- If an unloading or reloading curve exceeds the maximum past strain and intersects the backbone curve, it follows the backbone curve until the next reversal.

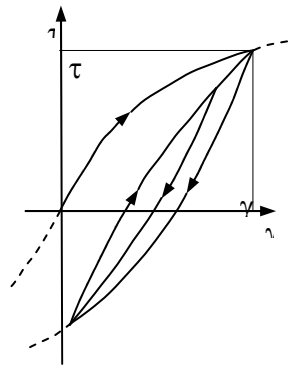

Fig. 2.7. Extended Masing Rules for Cyclic Stress-Strain Behavior [14]

Damping of soil in seismic loading can be computed based on the shear modulus ratio, $G/G_{\max}$. Ishihara and Zhang [10] also developed an empirical expression Eq. (2.4.9) for calculating the damping ratio λ of plastic and non-plastic soils. For the unloading or reloading, the modulus ratio $G/G_{\max}$ is calculated by the strain $(\gamma - \gamma_r)$/2.

$$\lambda = \frac{0.333(1+e^{-0.0145PI^{1.3}})}{2}\left\{0.586\left(\frac{G}{G_{\max}}\right)^2 - 1.547\left(\frac{G}{G_{\max}}\right) + 1\right\} \qquad (2.4.9)$$

The constitutive laws presented above are implemented in a two-dimensional finite element code. Even though the expression of the equations is complex, only the initial shear modulus $G_{\max}$ and the plastic index PI are needed for the input soil properties. The soil properties are also assumed as homogenous in two dimensions. The element shear modulus and the damping ratio are determined by the shear strain of the element at each time step.

Computer Code Implementation

The computer code was built from the software framework developed at the Open System for Earthquake Engineering Simulation (OPENSEES, http://opensees.berkeley.edu/). The constitutive laws presented above are implemented into a 2-dimensional 4-node plane strain element. This element was coded by C++ language and added into the system of Open System for Earthquake Engineering Simulation (OpenSees). OpenSees developed by PEER (2000) is a software framework for creating models and analysis methods to simulate structural and geotechnical systems in earthquake loading. The soil properties for the model are assumed as homogenous in two dimensions. The element shear modulus and the damping ratio are determined by the shear strain of the element at each time step. An iterative process in each increment is performed until the shear modulus and the damping ratio are compatible with the shear strain level. Even though the expression of the equations above is complex, only the initial shear modulus $G_{\max}$ and the plastic index PI are needed for the input soil properties.

2.5. Results of nonlinear response analysis for A1466-RW and A1466-CH models:

Fig. 2.8 shows three soil response profiles - the maximum shear strain versus depth, the minimum G/G_{max} versus depth and the maximum damping versus depth in the analysis. From the maximum shear strain versus depth profile (Fig. 2.8a), it shows that the maximum shear strains of soil elements below 100m are

less than 4×10^{-4}. The confining pressure is at least 1000 kPa below this depth. Based on Fig. 2.8.a, the sandy soil at this strain level doesn't show much modulus degradation and is still in elastic range (Fig. 2.8.b) and small damping is used in the analysis (Fig. 2.8.c). However, when the experimental curves, such as Vucetic and Dobry's curves [17], are used, the soils at this strain level still have large modulus degradation and corresponding larger damping is used in the analysis. Therefore, ignoring the influence of confining pressure on site response analysis will significantly underestimate the ground response in deep soil sites.

The Fig. 2.8a also shows that large strain - more than 10^{-3} strain was induced at the near surface soils (<80m depth). These shallow soils consist of silts, sands and low plastic soil that have high potential for liquefaction. Therefore, the surface soil may liquefy in the analyses. More damping may be involved in the site response analysis in the process of excess pore water pressure generation and large strain. This effect should be incorporated in the soil model in future work.

The study site is located in the New Madrid rift complex at 10.9 km away from the faults. The rock motions generated at this site have significant near field components. For the chosen motion, the displacement time history is given in Fig. 2.9(a). It shows an apparent pulse followed by 0.1m flings. However, the near field effect is not significant at the surface motion. After wave propagation through the 600m-soil column, the fling effect is not present in the displacement time history and the pulse is not significant, as seen in Fig. 2.9(b). These preliminary findings are in agreement with the lack of evidence of surface ground rupture due to previous earthquakes in the NMSZ.

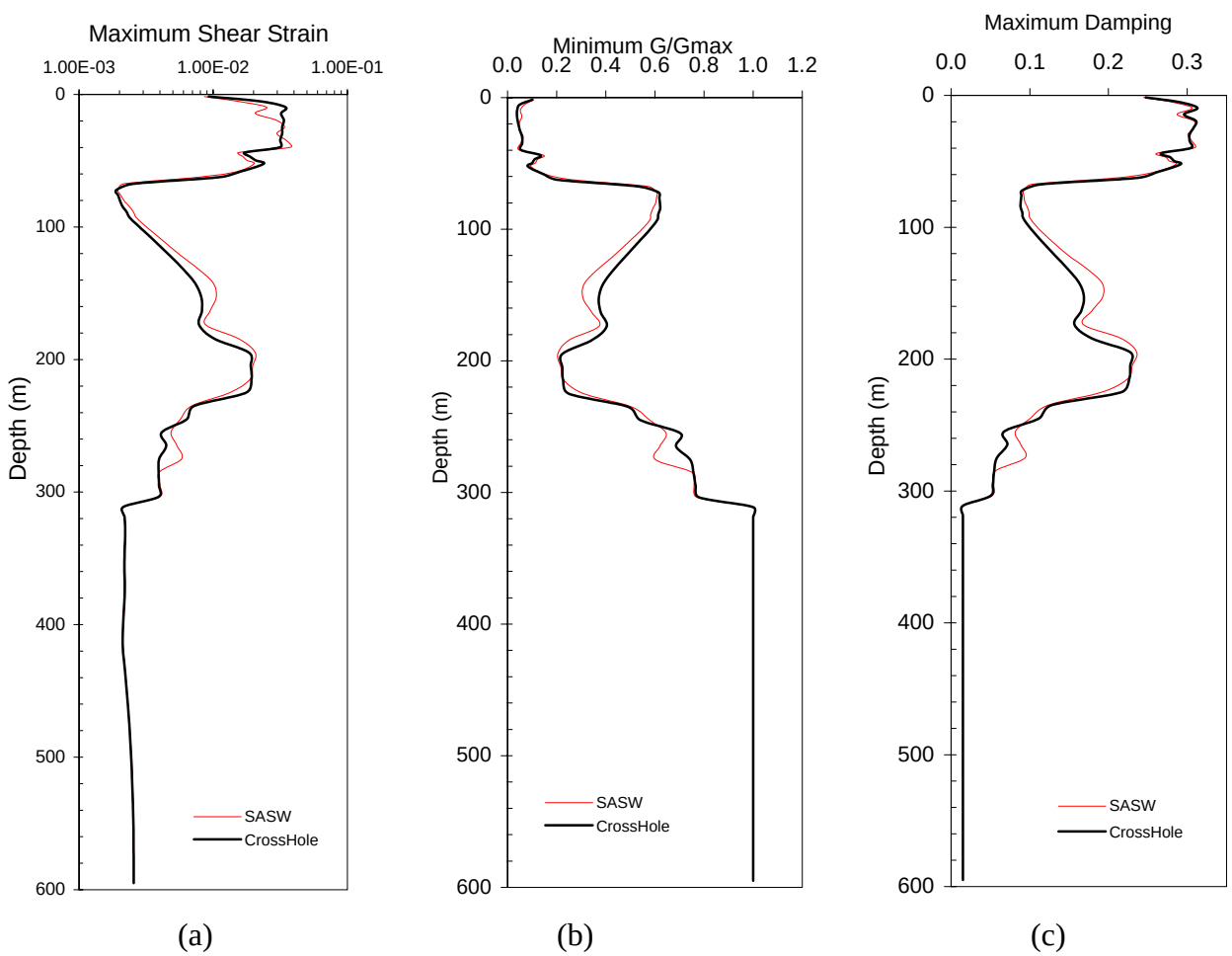

Fig. 2.8. Soil Response Profiles (a) Max. Shear Strain vs. Depth, (b) Min. G/G_{max} vs. Depth, (c) Max. Damping vs. Depth

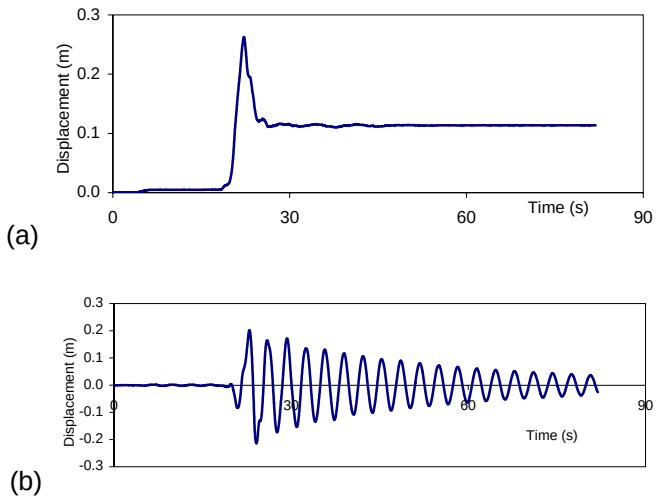

Fig. 2.9. Displacement Time History (a) Input Motion, (b) Surface Motion

These big deformations could explain extensive liquefaction phenomena observed during the earthquakes of 1811-1812 in New Madrid zone.

2.5.3. Response acceleration spectra:

Response acceleration spectra were computed for resulting time histories obtained from the analyses. These spectra are for free-field conditions using a damping value of 0.05. The spectra for the two types of soil profiles modeled are shown in Figures 2.10 and 2.11, for the shallow and deep soil profiles, respectively.

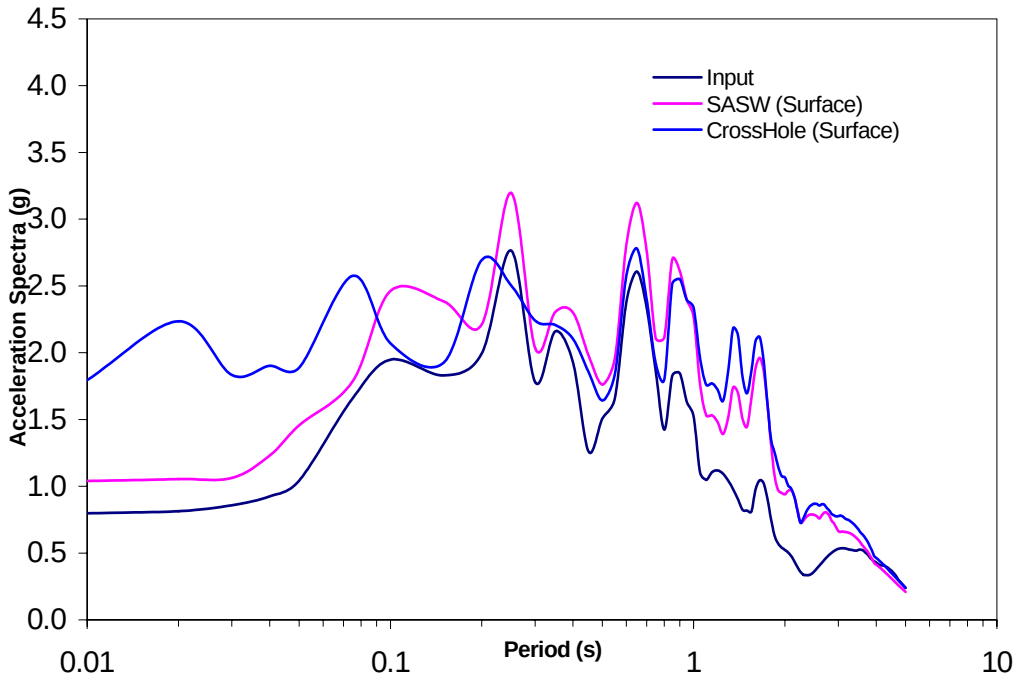

Figure 2.10. Response Spectra for Shallow (hypothetical) Soil Profile ~60m for the SASW and CH models using M=7.1 input synthetic motion (also shown)

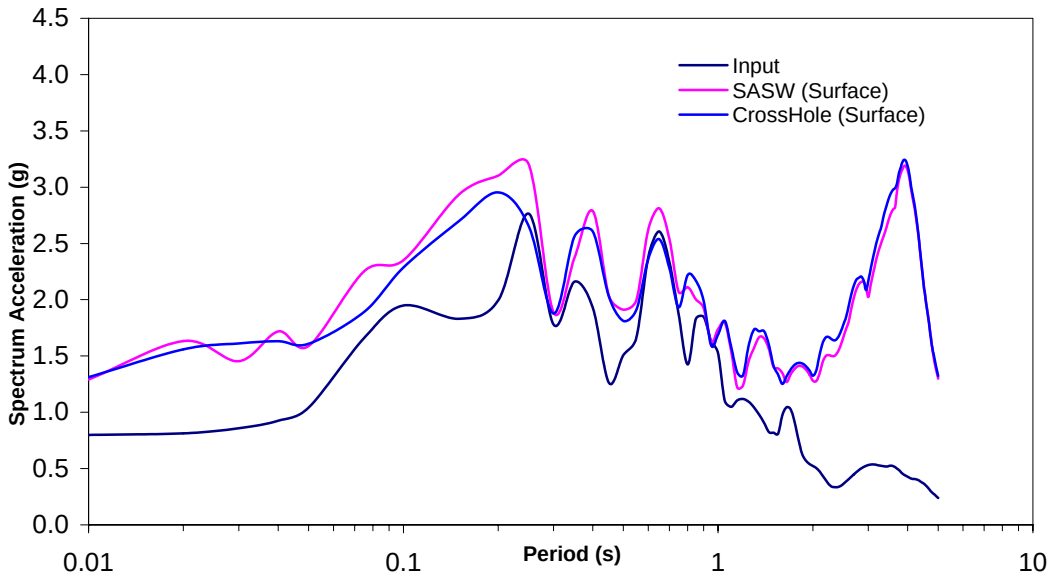

Figure 2.11. Response Spectra (5% damping) for Deep Soil profile the SASW and CH models using M=7.1 input synthetic motion (also shown)

Conclusions

Analyses were carried out for soil profiles modeled using geophysical techniques. The engineering significance of the data is obtained based on the impact on the analyses. This is assessed by processing

the data in a modern ground response analysis at both linear and non-linear levels of strain. Even though the synthetic ground motions are indicative of high frequency content motion, the trends in the similarity of response spectra are noticeable. Further work is required to assess the need to filter out some of the artificial high frequency content.

The results from nonlinear ground response analysis for the NMSZ shallow soil profile with a thickness of about ~60m show small differences in the ground response analysis. There only a small significant difference in the response spectra at the periods from 0.5 and 1.5. Most of the differences are seen in the periods less that 0.5 sec., which tend to be of little significance for bridges and possibly an artificial product of the synthetic motions. For a deep soil profile those differences are even less pronounced and comparisons between the SASW and CH data are difficult to identify.

Comparison of response spectra from different source generated synthetics, show that the results obtained using synthetics generated by a point source model with H=650m are close to those obtained using synthetics generated by composite source model for the same magnitude. The advantages of using high quality cross-hole data for use in ground response are not justified. SASW surface geophysics results tend to satisfy the engineering requirements for ground response analysis. However, for shallower deposits and more intrinsic soil-structure interaction analysis the CH geophysical characterization may be justified.

References

1. Anderson, N., Chen, G., Kociu, S., Luna, R., and Malovichko, A., Malovichko, D., Shylakov, D (2003) Vertical shear-wave velocity profiles generated from the spectral analysis of surface waves (SASW technique): Field examples from six bridge sites in southeast Missouri. UMR Department of Geology & Geophysics Prepared for MoDOT
2. Boore, D.B. (1996) SMSIM FORTRAN Program for Simulating Ground Motions from Earthquakes: Version 1.0. USGS Open File Report 96-80-A
3. FEMA 368 http://bssconline.org/NEHRP200/comments/provisions
4. FEMA 369 http://bssconline.org/pubs/downloads.html
5. Herrmann, R. B., Julia-Casas, J., Rix, G., Akinci, A., Bodin, P., and C.J.Ammon Shear-wave velocity estimates for deep soils of the Mississippi embayment from the inversion of teleseismic receiver functions http://www.eas.slu.edu/People/RBHerrmann/EMBAYRFTN.0113/
6. Herrmann, R.B., and A.Akinci.Mid-America Ground Motion Models http://www.eas.slu.edu/People/RBHermann/MAEC/maecgnd.html
7. Hoffman, D., (2003) MoDNR, Geological Survey Program (February 27,2003)
8. Idriss, I. M.(1990a). "Response of Soft Soil Sites During Earthquakes." In Proceedings of the Symposium to Honour Professor H. B. Seed, Berkeley.
9. Idriss, I. M. (1990b). "Influence of Local Site Conditions on Earthquake Ground Motions." In Proceedings of the 4th U.S. National Conference on Earthquake Engineering, Palm Springs, Vol. 1, pp. 55-57.
10. Ishihara, I. and Zhang, X. (1993). “Unified Dynamic Shear Moduli and Damping Ratios of Sand and Clay,” Soils and Foundations, Vol. 33, No. 1, 182-191.
11. Khalil, M.A.K., (1996), Uncovering Hidden Earthquake Hazards in the Continental United States: The American Physical Society, 1-8.
12. Kondner,R.L., and Zelasko,J.S.(1963).“A hyperbolic Stress-Strain Formulation for Sands“ Proceedings,2nd Pan American Conference on Soil Mechanics and Foundations Engineering,

289- 324

13. Liu, Hsi-Ping, Yiquang Hu, James Dorman, Tzyy-Shiou Chang, Jer-Ming Chiu (1997) Upper Mississippi embayment shallow seismic velocities measured in situ, Engineering Geology 46 (1997), 313-330
14. Masing, G., “Eigenspannungen und Verfestigung Beim Messing,” Proceedings, 2nd International Congress of Applied Mechanics, Zurich, Switzerland, 1926
15. National Seismic Hazard Mapping Program .http://geohazards.cr.usgs.gov/eq/html/nehrp.html
16. Newmark, N. M. (1959). “A Method of Computation for Structural Dynamics,” Journal of Geotechnical Engineering Division, ASCE, 85, 67-94.
17. Vucetic, M., and Dobry, R. (1991). “Effect of Soil Plasticity on Cyclic Response,” Journal of Geotechnical Engineering, ASCE, 117(1), 89-107.
18. Zheng, W. and Luna, R., (2004), “Nonlinear Site Response Analysis in the New Madrid Seismic Zone”, to appear in the Proceedings: 5th International Conference in Case Studies in Geotechnical Engineering, April, New York City.